Final Technical Report

Project Title: A Biomimetic Approach to New Adsorptive Hydrogen Storage Metal-Organic Frameworks

Recipient: Texas A&M Research Foundation

Principal investigator: Hong-Cai (Joe) Zhou

Address: Dept. of Chem., Texas A&M University, College Station, TX 77842-3012

Phone: (979) 845-4034

Email: zhou@chem.tamu.edu

DOE Managers

HQ: Ned Stetson

Phone: (202) 586-9995

Email: Ned.Stetson@ee.doe.gov

GO: Jesse Adams

Phone: (720) 356-1421

Email: Jesse.Adams@go.doe.gov

Contract Number: DE-FC36-07GO17033

Project Start Date: July 1, 2007

Project End Date: June 30, 2013

Date of Report: September 30, 2013

This report does not contain any proprietary, confidential, or otherwise restricted information

Executive summary

In the past decades, there has been an escalation of interest in the study of MOFs due to their fascinating structures and intriguing application potentials. Their exceptionally high surface areas, uniform yet tunable pore sizes, and well-defined adsorbate-MOF interaction sites make them suitable for hydrogen storage. Various strategies to increase the hydrogen capacity of MOFs, such as constructing pore sizes comparable to hydrogen molecules, increasing surface area and pore volume, utilizing catenation, and introducing coordinatively unsaturated metal centers (UMCs) have been widely explored to increase the hydrogen uptake of the MOFs. MOFs with hydrogen uptake approaching the DOE gravimetric storage goal under reasonable pressure but cryo-temperature (typically 77 K) were achieved. However, the weak interaction between hydrogen molecules and MOFs has been the major hurdle limiting the hydrogen uptake of MOFs at ambient temperature.

Along the road, we have realized both high surface area and strong interaction between framework and H_2 are equally essential for porous materials to be practically applicable in H_2 storage. Increasing the isosteric heats of adsorption for H_2 through the introduction of active centers into the framework could have great potential on rendering the framework with strong interaction toward H_2. Approaches on increasing the surface areas and improving hydrogen affinity by optimizing size and structure of the pores and the alignment of active centers around the pores in frameworks have been pursued, for example: (a) the introduction of coordinatively UMC (represents a metal center missing multiple ligands) with potential capability of multiple dihydrogen-binding (Kubas type, non-dissociative) per UMC, (b) the design and synthesis of proton-rich MOFs in which a H_3^+ binds dihydrogen just like a metal ion does, and (c) the preparation of MOFs and PPNs with well aligned internal electric fields.

We believe the accomplishments of this DOE supported research will greatly benefit the future pursuit of H_2 storage materials. The ultimate goal to increase the gravimetric and volumetric hydrogen storage capacity to meet DOE targets for Light-Duty Vehicles is achievable.

1. Project Approaches

This project pursued combined approaches to develop sorption based hydrogen storage materials operable at ambient temperatures and applicable pressures. The objective of this multiple-year research aims at synthesis, characterization, and validation of innovative hydrogen storage materials that meet or exceed DOE's system targets by improving the hydrogen-affinity, porosity, stability, and density of sorbents. The project addressed molecular design based on fundamental understanding of H_2-sorbent interaction to achieve high hydrogen storage capacity. Novel approaches to improve the practical performance qualities of the sorbents have been emphasized.

Our approaches to enhance H_2 uptake have been summarized as follows:

(1) Prepare the catenation isomer pair to evaluate the contribution from catenation to the hydrogen uptake of a MOF material. Catenation can be utilized to reduce pore sizes in porous MOFs and has also been explored as an efficient method to improve the hydrogen uptake of MOFs.

(2) Synthesize porous MOFs with high hydrogen adsorption capacities based on different coordinatively UMCs. The implementation of coordinatively UMCs into porous MOFs has been considered as one of the most effective ways to improve their affinities to hydrogen.

(3) Hydrogen storage studies in MOFs containing nanoscopic cages based on double-bond-coupled di-isophthalate linkers. Those ligands containing phenyl rings in MOFs have been proved favorable for hydrogen adsorption.

(4) Design and synthesize porous MOFs based on an anthracene derivative which can provide additional hydrogen binding sites to increase the hydrogen uptake.

(5) Systematically study the stable MOFs with high surface areas by the incorporation of mesocavities and microwindows.

(6) Construct MOFs with "close-packing" alignment of open metal sites, which can increase the number of nearest neighboring open metal sites of each H_2-hosting void in a three-dimensional (3-D) framework so that they can interact effectively with the guests (H_2 molecules) inside the void.

(7) Prepare an unprecedented linkage isomer pair of MOFs and study the impact of pore size on H_2 storage capacity in MOFs.

(8) Incorporate polyyne unit into MOFs, which has higher H_2 affinity.

(9) Tune the pore structure by introducing difference functional groups into MOFs to study the effect on H_2 uptake.

(10) Construct stable and high-surface-area Zr-MOFs, study the effect on gas uptake by introducing different metals into their porphyrin linkers.

(11) Design and synthesize PPNs with high chemical stability suitable for further decoration.

(12) Incorporate metal ions into PPNs, which can enhance the isosteric heats of hydrogen-adsorption.

(13) Ligand truncation strategy for enhanced H_2 adsorption.

(14) Construct MOFs from a highly conjugated ligand exhibiting a high hydrogen uptake capacity.

(15) Build up porous lanthanide MOFs and studied their potential application in gas adsorption.

2. Project Objectives

All attempted approaches are to increase the surface areas and improving hydrogen affinity by optimizing size and structure of the pores and the alignment of active centers around the pores in frameworks, specifically objectives:

(1) Enhance the hydrogen isosteric heat of adsorption (Q_{st}) of MOFs (please refer to the top of each page for frequently used abbreviations in this proposal) and/or PPNs to 15~20 kJ/mol by: (a) the introduction of coordinatively UMC (represents a metal center missing multiple ligands) with potential capability of multiple dihydrogen-binding (Kubas type, non-dissociative) per UMC, (b) the design and synthesis of proton-rich MOFs in which a H_3^+ binds dihydrogen just like a metal ion does, and (c) the preparation of MOFs and PPNs with well aligned internal electric fields;

(2) Increase the gravimetric hydrogen storage capacity to 0.055 kg H_2/kg at 295 K by reaching Objective 1 while maintaining high porosity of the sorbent;

(3) Increase the volumetric hydrogen storage capacity to 0.040 kg H_2/L at 295 K by achieving Objectives 1 and 2 while improving the density of the sorbent.

3. Summary of Project Accomplishments

Table 1. Technical System Targets: On-Board Hydrogen Storage for Light-Duty Vehicles

Storage Parameter	Units	2010	2017	Ultimate
System Gravimetric Capacity: Usable, specific-energy from H_2 (net useful energy/max system mass)	kWh/kg (kg H_2/kg system)	1.5 (0.045)	1.8 (0.055)	2.5 (0.075)
System Volumetric Capacity: Usable energy density from H_2 (net useful energy/max system volume)	kWh/L (kg H_2/L system)	0.9 (0.028)	1.3 (0.040)	2.3 (0.070)

Table 2. Revised High Pressure Data of Selected materials developed by TAMU

	Excess (kg/kg)	Excess (kg/L)	Total' (wt%)	Total' (kg/L)	Density (g/cm^3)	T (K)	P (bar)	Langmuir (BET) m^2/g
PCN-6	0.0720	0.0402	7.2	0.0411	0.528*	77	50	3800
PCN-6'	0.0420	0.0118	4.4	0.0140	0.292*	77	50	2700
PCN-10	0.0453	0.0332	4.3	0.0348	0.767*	77	20	1779 (1407)
PCN-11	0.0532	0.0378	5.1	0.0406	0.749*	77	20	2442 (1931)
PCN-12	0.0594	0.0457	5.7	0.0496	0.814*	77	50	2425(1943)
PCN-12'	0.0265	0.0236	3.1	0.0293	0.910*	77	50	1962(1577)
PCN-14	0.0462	0.0366	4.7	0.0433	0.871*	77	50	2176 (1753)
PCN-16	0.0537	0.0417	5.5	0.0451	0.778*	77	45	2800 (2273)
PCN-16'	0.0299	0.0246	3.3	0.0320	0.943*	77	30	2200 (1760)
PCN-20	0.0661	0.0327	7.1	0.0358	0.466*	77	50	4237 (3525)
PCN-26	0.0294	0.0264	3.3	0.0301	0.897*	77	30	2545(1854)
PCN-46	0.0561	0.0347	6.1	0.0434	0.663*	77	32	2800 (2500)
PCN-50	0.0465	0.0232	5.4	0.0298	0.524*	77	45	4523 (3678)
PCN-53	0.0440	0.0250	5.7	0.0364	0.600*	77	45	(2817)
PCN-61	0.0624	0.0350	6.3	0.0403	0.597*	77	33	3500 (3000)
PCN-66	0.0666	0.0296	7.7	0.0394	0.470*	77	45	4600 (4000)
PCN-68	0.0777	0.0296	8.5	0.0372	0.402*	77	44	6033 (5109)
PCN-69	0.0551	0.0204	7.2	0.0289	0.371*	77	50	6268 (3806)
PCN-80	0.0471	0.0300	6.2	0.0424	0.643*	77	50	4150 (3850)
PPN-305	0.0560	0.0409	5.5	0.0425	0.730*	77	24	2599(1720)
PPN-1	0.0341	0.0043	3.3	0.0042	0.126**	77	45	827(1249)

PPN-2	0.0389	0.0035	4.8	0.0045	0.089**	77	50	2790 (1764)
PPN-3	0.0428	0.0083	5.4	0.0112	0.194**	77	42	5323 (2840)
PPN-4	0.0910	0.0258	11.8	0.0379	0.283**	77	55	10400(6400)
PPN-4	0.0118	0.0033	3.1	0.0090	0.283**	295	90	10400(6400)

*crystal density; **density of simulated structure

4. Specification of Selected Accomplishments

(1) Prepared the catenation isomer pair to evaluate the contribution from catenation to the hydrogen uptake of a MOF material.

Catenation, the intergrowth of two or more identical frameworks, has long been an interesting topic in MOF research. It can be utilized as an alternative way to reduce pore sizes in porous MOFs and has also been explored as an efficient method to improve the hydrogen uptake of MOFs. Recently, we developed a templating strategy to control catenation/noncatenation in porous MOFs, obtained the catenation isomer pair of PCN-6 and PCN-6', and were able to quantitatively evaluate the contribution from catenation to the hydrogen uptake of a MOF material (Figure 1). Our studies revealed that catenation can lead to a 41% improvement of apparent Langmuir surface area (3800 m^2/g for PCN-6 vs 2700 m^2/g for PCN-6′), a 29% increase in excess gravimetric hydrogen uptake (1.74 wt% for PCN-6 vs 1.35 wt% for PCN-6′) at 77 K/760 torr, and a 133% increase in volumetric hydrogen uptake (9.19 kg/m^3 for PCN-6 vs 3.49 kg/m^3 for PCN-6′) in the

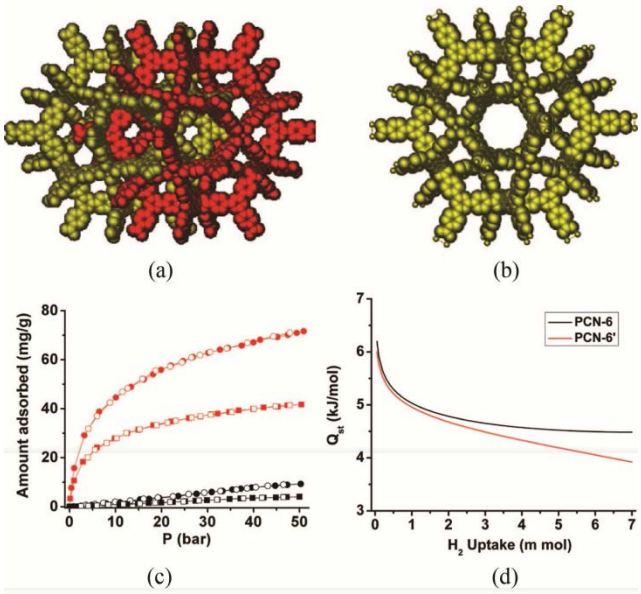

Figure 1. (a) The framework of catenated PCN-6. (b) The framework of noncatenated PCN-6'. (c) Excess hydrogen sorption isotherms of PCN-6 and PCN-6' at 77 (red) and 298 K (black): circles, PCN-6; squares, PCN-6'; solid symbols, adsorption; open symbols, desorption. (d) Isosteric heats of adsorption for PCN-6 and PCN-6′.

catenation isomer pair of PCN-6/PCN-6′. The study of isosteric heats of adsorption indicated that catenated PCN-6 and noncatenated PCN-6′ have similar hydrogen-adsorption enthalpies at low coverage (6.2 kJ/mol for PCN-6 vs 6.0 kJ/mol for PCN-6′). However, as the hydrogen load increases, PCN-6 exhibits steadily higher hydrogen-adsorption enthalpies than those of PCN-6′. INS spectroscopy studies revealed that the first sites occupied by H_2 are the open Cu centers of the paddlewheel units in both PCN-6 and PCN-6′. However, in PCN-6, there exist three specific H_2-binding Cu sites while PCN-6′ possesses only one. At high hydrogen loadings, the interaction between H_2 molecules and the organic linkers is stronger in catenated PCN-6 than that in noncatenated PCN-6′. Such a stronger interaction resulted in more effective hydrogen binding sites in catenated PCN-6. Hydrogen sorption studies up to 50 bar demonstrated that catenation can lead to higher hydrogen uptake in MOFs even at high pressure. For example, the excess hydrogen uptake of catenated PCN-6 is 72 mg/g (6.7 wt %) at 77 K/50 bar or 9.3 mg/g (0.92 wt %) at 298 K/50 bar, and that in noncantenated PCN-6' is 42 mg/g (4.0 wt %) at 77 K/50 bar or 4.0 mg/g (0.40 wt %) at 298 K/50 bar. Importantly, PCN-6 exhibits a total hydrogen uptake of 95 mg/g (8.7 wt %) (corresponding to 53.0 g/L) at 77 K/50 bar and 15 mg/g (1.5 wt %) 298 K/50 bar. Significantly, the deliverable hydrogen capacity of PCN-6 is 75 mg/g (or 41.9 g/L) at 77 K/50 bar, showing its great potential as a cryogenic hydrogen-storage medium.

In conclusion, catenation can be utilized to reduce pore sizes in porous MOFs and has also been explored as an efficient method to improve the hydrogen uptake of MOFs.

(2) Synthesized porous MOFs with high hydrogen adsorption capacities based on different coordinatively UMCs.

The implementation of coordinatively UMCs into porous MOFs has been considered as one of the most attractive ways to improve their affinities to hydrogen. Recent theoretical calculations suggested that the H_2-open metal center interactions may be tuned by varying the metal types, and the evaluation of different UMCs' affinities to hydrogen molecules will be very instructive for the future design of porous MOFs with high hydrogen adsorption capacities, especially at near ambient temperatures. Herein, we prepared three isostructural porous MOFs, designated as PCN-9 (Co), PCN-9 (Fe)

and PCN-9 (Mn), respectively. To test the permanent porosities of the three porous MOFs, N_2 sorption isotherms were measured at 77 K. All of them exhibit type-I sorption behavior, as expected for microporous materials. Derived from the N_2 sorption data, the Brunauer-Emmett-Teller (BET) surface areas are 1064 m^2/g (Langmuir surface area, 1355 m^2/g), 682 m^2/g (Langmuir surface area, 848 m^2/g), and 836 m^2/g (Langmuir surface area, 1057 m^2/g) for PCN-9 (Co), PCN-9 (Fe), and PCN-9 (Mn), respectively. H_2 sorption measurements at 77 K were also carried out to check their hydrogen storage performances. At 77 K and 760 Torr, the hydrogen uptake capacity of PCN-9 (Co) is 1.53 wt %, and PCN-9 (Fe) can adsorb 1.06 wt % hydrogen, while PCN-9 (Mn) can uptake 1.26 wt % hydrogen. The H_2 affinities of the three porous MOFs have been estimated by isosteric heats of adsorption Qst. PCN-9 (Co) has a Qst of 10.1 kJ/mol and PCN-9 (Mn) has a Qst of 8.7 kJ/mol, while PCN-9 (Fe) has a relatively lower Qst of 6.4 kJ/mol. These results revealed that the Co UMC possesses a higher hydrogen affinity compared to the Fe and Mn UMCs, indicating that the implementation of open Co centers into porous MOFs may be a promising way to enhance hydrogen adsorption enthalpies for near-ambient hydrogen storage application.

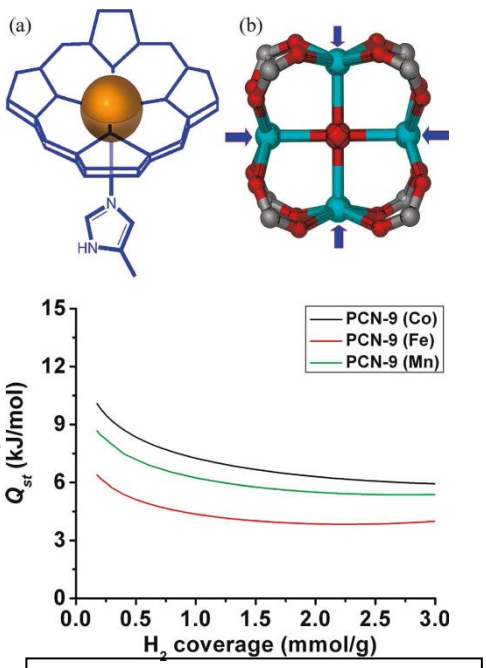

Figure 2. (a) The active center of hemoglobin (the orange sphere represents an Fe atom). (b) The $M_4(\mu 4\text{-}O)(carboxylate)_4$ SBU, with arrows indicating the displaced entatic metal centers (M=Co, Fe, Mn).
Bottom: Isosteric heats of adsorption of H_2 in PCN-9s.

In conclusion, the implementation of coordinatively UMCs into porous MOFs has been carried out and it is one of the most attractive ways to improve their affinities to hydrogen.

(3) Hydrogen storage studies in MOFs containing nanoscopic cages based on double-bond-coupled di-isophthalate linkers.

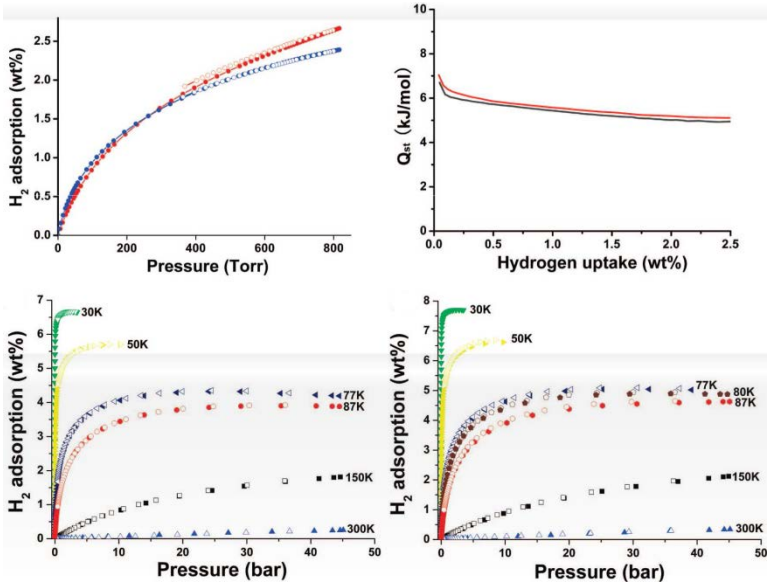

Figure 3: Top left: H_2 adsorption isotherms for PCN-10 (blue) and PCN-11 (red) at 77 K; top right: Isosteric heats of hydrogen adsorption of PCN-10 (blue) and PCN-11 (red); bottom left: Excess adsorption isotherms of PCN-10 at multiple temperatures; bottom right: Excess adsorption isotherms of PCN-11 at multiple temperatures.

While ligands containing phenyl rings have been proven favorable for hydrogen adsorption, those containing double-bond functionalities have rarely been studied in gas adsorption in MOFs. Herein, we present hydrogen storage studies in MOFs containing nanoscopic cages based on two predesigned double-bond-coupled bis(isophthalate) ligands: azobenzene-3,3′,5,5′-tetracarboxylate (abtc) and transstilbene-3,3′,5,5′-tetracarboxylate (sbtc). Solvothermal reactions of $Cu(NO_3)_2$ with H_4aobtc or H_4sbtc give rise to isostructural PCN-10 and PCN-11, respectively. The enduring porosity of PCN-10 and PCN-11 is confirmed by gas adsorption studies. The N_2 adsorption isotherms of the activated samples exhibit type-I sorption behavior with a Langmuir surface area of 1779 or 2442 m^2/g, corresponding to a BET surface area of 1407 or 1931 m^2/g and a total pore volume of 0.67 or 0.91 mL/g for PCN-10 or PCN-11, respectively. In particular, both contain nanoscopic cages that are particularly suitable for gas storage. At 760 Torr and 77 K, the excess hydrogen uptake of PCN-10 is 2.34 wt % (18.0 g/L) and that of PCN-11 is as high as 2.55 wt % (19.1 g/L). When the pressure is increased, the excess adsorption at 77 K saturates around 20 atm and reaches values of 4.33% (33.2 g/L) and 5.05% (37.8 g/L) for PCN-10 and PCN-11, respectively.

In conclusion, gas adsorption experiments suggest that MOFs containing C=C double bonds are more favorable than those with N=N double bond in retaining porosity after thermal activation, although the N=N double bond has slightly higher H_2 affinity.

(4) Design and synthesize porous MOFs based on an anthracene derivative which can provide additional hydrogen binding sites to increase the hydrogen uptake.

Although the inorganic metal clusters of porous MOFs were considered as the initial hydrogen binding sites with successive adsorption sites by INS (inelastic neutron scattering) and NPD (neutron powder diffraction) studies, increasing the aromaticity of the organic linkers has also been theoretically predicted and experimentally proven to be an effective way to improve hydrogen adsorption capacities of porous MOFs. Based on this issue, we designed a new ligand, adip, (H_4adip = 5,5'-(9,10-anthracenediyl)di-isophthalate) and found that the central anthracene can provide additional hydrogen binding sites to increase the hydrogen uptake (Figure 4).

Under solvothermal conditions, reactions of H_4adip with $Cu(NO_3)_2$ gave rise to a porous MOFs, designated as PCN-14. Single crystal X-ray analysis revealed that PCN-14 adopt the $Cu_2(COO^-)_4(H_2O)_2$ paddlewheel as the SBUs. The Cu-Cu distance is 2.654 Å, and the Cu-aqua distance is 2.122 Å for the paddlewheel SBU found in PCN-14. The structure of PCN-14 consists of nanoscopic cages, each with a volume of 1150 $Å^3$. N_2 sorption analysis revealed that PCN-14 retains its permanent porosity and has a BET surface area of 1753 m^2/g. The high porosity and nanoscopic cages in PCN-14 encouraged us to evaluate its hydrogen adsorption performance. At 77 K and 760 Torr, the excess gravimetric hydrogen uptake capacity of PCN-14 can reach 2.70 wt %, which is among the highest of reported MOFs under similar conditions. At higher pressure, the excess gravimetric hydrogen uptake of PCN-14 reaches saturation with a value of 4.42 wt %.

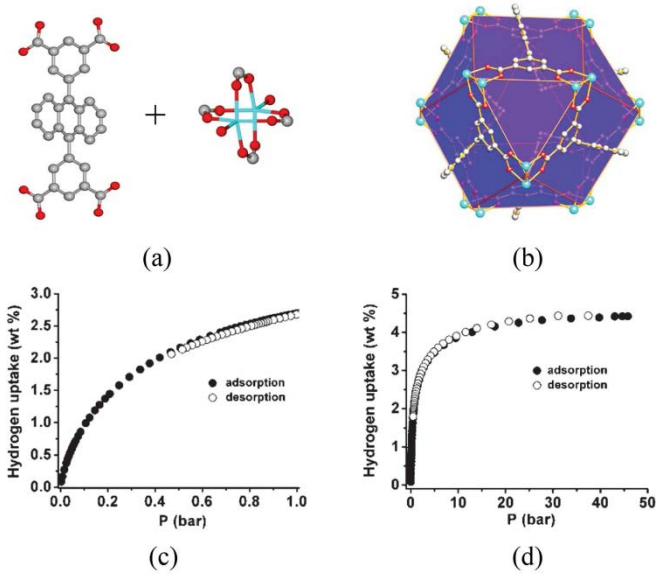

Figure 4: (a) The adip ligand and $Cu_2(COO\text{-})_4(H_2O)_2$ paddlewheel SBU. (b) Nanoscopic cage in PCN-14. (c) Low-pressure H_2 sorption isotherms of PCN-14 at 77 K. (d) High-pressure excess H_2 sorption isotherms of PCN-14 at 77 K.

This corresponds to a volumetric uptake of 36.6 g/L calculated using the crystal density of dehydrated PCN-14 (0.829 g/cm^3).

Though the ultimate sorption capacity is lower than similar Cu-MOFs because of the smaller effective surface area, the nanoscopic cages permit a more effective potential overlap near the Cu^{2+} site, leading to the relatively higher initial Qst of 8.6 kJ/mol.

(5) Obtained stable MOFs with high surface areas by the incorporation of mesocavities and microwindows.

It has been well established that the high pressure gravimetric hydrogen adsorption capacity of a MOF is directly proportional to its surface area. However, MOFs of high surface areas tend to decompose upon activation. In our previous work, we've described an approach toward stable MOFs with high surface areas by incorporating mesocavities with microwindows. To extend this work, herein we present an isoreticular series of (3,24)-connected MOFs made from dendritic hexa-carboxylate ligands (Figure 5). In order to test the framework stability, nitrogen sorption measurements were carried out in fully activated PCN-68 and PCN-610. In PCN-68, a dramatic increase of nitrogen sorption has been observed (Figure 5d). The BET surface area calculated based on the low pressure region data can reach as high as 5109 m^2/g, with a Langmuir surface area of 6033 m^2/g.

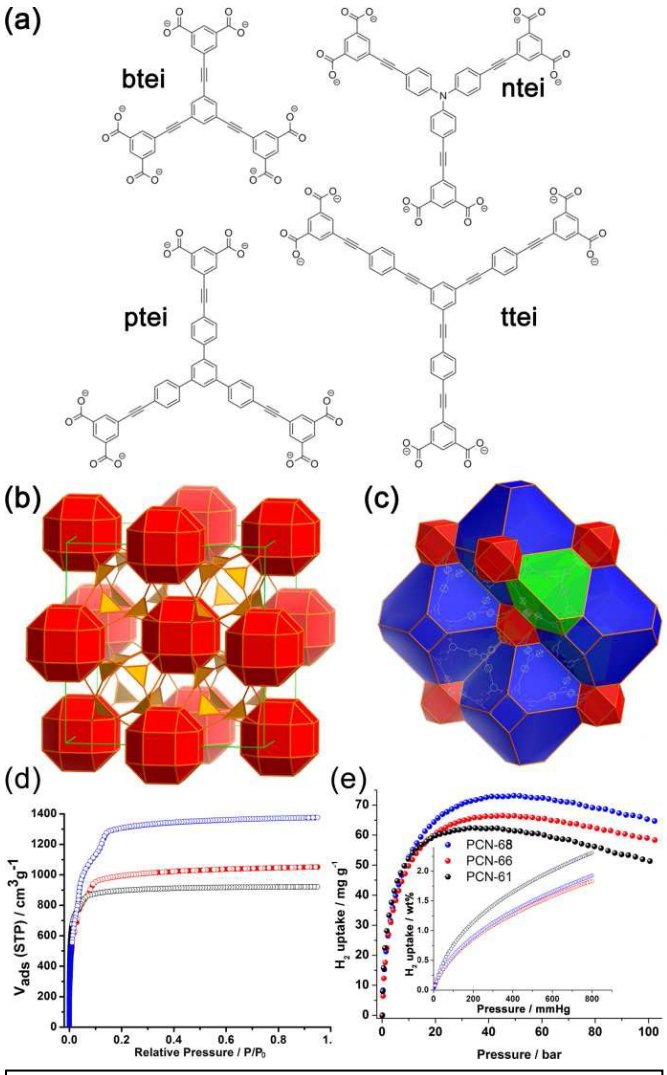

Figure 5. (a) Nanoscopic ligands btei (PCN-61), ntei (PCN-66), ptei (PCN-68) and ttei (PCN-610). (b) (3,24)-Connected network in PCN-68. (c) 3D polyhedra packing in PCN-68. (d) N_2 sorption isotherms of PCN-61, PCN-66, and PCN-68 at 77 K. (e) Gravimetric H_2 uptakes in PCN-6X series at 77 K.

To the best of our knowledge, PCN-68 possesses the one of the highest surface area reported for MOFs based on paddlewheel clusters, and it is also among the highest reported.

The hydrogen uptake capacities of PCN-6X series are shown in Figure 5e. At a low pressure region (< 1 bar), the hydrogen uptake capacity is mainly controlled by the hydrogen affinity towards the framework, which can be quantified by the isosteric heat of adsorption. PCN-61, which has the smallest pore size, also has the highest heat of adsorption and highest capacity (2.25 wt % at 77 K, 1 bar). PCN-66 and PCN-68 have heats of adsorption and adsorption capacities similar to each other (1.79 wt % in PCN-66 vs. 1.87 wt % in PCN-68). This trend is consistent with the nature of physisorption, in which narrower pores would have stronger interactions with the guest gas molecules due to the increased interaction between the guests and the opposite potential walls within small pores. Unlike the low pressure hydrogen sorption capacity, which is dominated by the hydrogen affinity, the maximum excess hydrogen uptake capacity in MOFs, which typically can only be reached at high pressure range, is controlled mainly by the surface area and pore volume. This is consistent with what has been observed in the PCN-6X series. As can be seen from Figure 5e, PCN-68, which has the highest surface area, also has the highest maximum excess hydrogen uptake capacity (7.2 wt%), which makes it one of the best adsorbents with the highest gravimetric hydrogen uptake capacity. It is worth noting that the maximum adsorption pressure increases from PCN-61 (33 bar) to PCN-66 (45 bar) and PCN-68 (50 bar), indicating higher pressure is needed to reach maximum adsorption in sorbents with higher pore volumes.

Using the crystal density data, the volumetric hydrogen uptake capacities were also calculated. Unlike the trend in gravimetric capacity, where the material with the highest surface area has the highest capacity, the volumetric capacity follows the opposite trend, which is dominated by the densities of the sorbents. The gravimetric capacity has been emphasized in the past hydrogen storage research, and rightfully so. However, the volumetric capacity is particularly relevant in volume-limited fuel-cell applications. Both of these criteria should be emphasized equally in the search for ideal hydrogen storage materials.

These high surface area MOFs provide us with an opportunity to incorporate additional open metal sites to increase the heat of adsorption of the framework and the density thus the volumetric storage capacity of the sorbent.

(6) Constructed MOFs with “close-packing” alignment of open metal sites for hydrogen storage.

Many efforts have been devoted to the enhancement of hydrogen affinity in MOFs, thus increasing hydrogen uptake, such as introducing framework interpenetration, constructing pores to fit the size of the hydrogen molecule, and the creation of open metal sites. However, our strategy to enhance H_2 uptake is to strengthen the H_2-MOF interaction by increasing the number of nearest neighboring open metal sites of each H_2-hosting void in a 3-D framework and to align the open metal sites so that they can interact directly with the guests (H_2 molecules) inside the void. Based on this issue, a ligand designed using such a strategy is 5,5’-methylene-di-isophthalate (mdip) and two Cu-mdip MOFs (PCN-12 and PCN-12') have been synthesized (Figure 6).

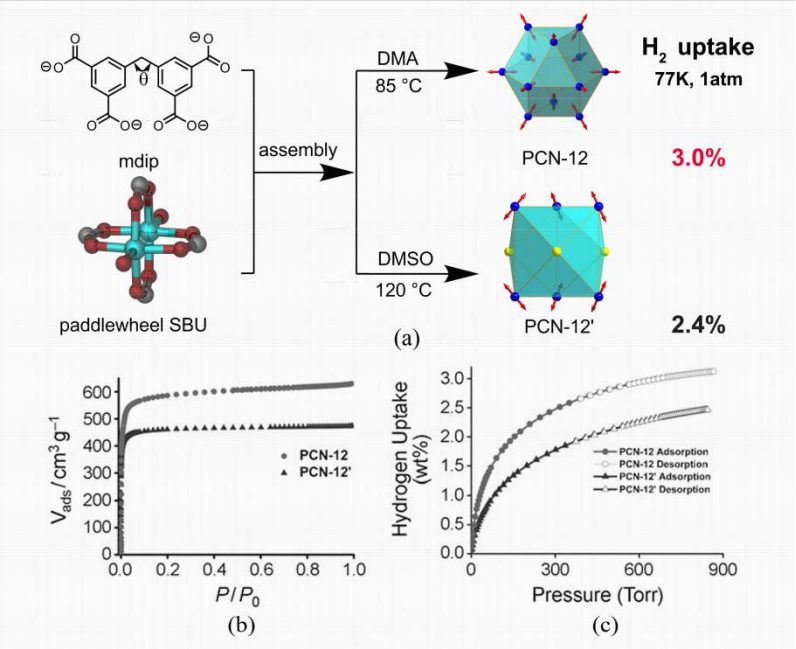

Figure 6. (a) The synthesis, open metal site alignment, and hydrogen uptake of the two MOF polymorphs: PCN-12 and PCN-12'. (b) N_2 adsorption isotherms for PCN-12 and PCN-12'. (c) H_2 adsorption isotherms for PCN-12 and PCN-12'.

PCN-12 adopts a dicopper paddlewheel motif as its SBU. The paddlewheel SBU occupies the 12 vertices of a cuboctahedron while 24 isophthalate motifs span all 24 edges. As expected, at the 12 corners of the cuboctahedron, there are 12 open copper-coordination sites pointing toward the center of the cage. Each square face is connected to another square face of a neighboring cuboctahedron through four mdip

bridges. Every cuboctahedron connects to six others in three orthogonal directions to form a 3-D net. However, in PCN-12' every mdip ligand has C_{2v} symmetry. Each of the six paddlewheels connects three mdip ligands in a trigonal-prismatic fashion with paddlewheel units occupying all corners of the “prism” and the three mdip ligands residing on the three sides. Evidently, the open metal coordination sites point away from the cavity of the polyhedron.

The nitrogen adsorption isotherms reveal that both PCN-12 and PCN-12' exhibit typical type-I adsorption behavior. The Langmuir surface area, BET surface area, and pore volume of PCN-12 are 2425 $m^2 g^{-1}$, 1943 $m^2 g^{-1}$, and 0.94 mLg^{-1}, respectively, whereas those for PCN-12' are 1962 $m^2 g^{-1}$, 1577 $m^2 g^{-1}$, and 0.73 mLg^{-1}, respectively. The hydrogen adsorption isotherm of PCN-12' shows a 2.40 wt% (20.4 gL^{-1}) hydrogen uptake at 77 K and 1 atm, comparable to those of other MOFs containing cuboctahedral cages. However, PCN-12 exhibits an exceedingly high hydrogen uptake of 3.05 wt% (23.2 gL^{-1}) under the same conditions. This high hydrogen uptake of PCN-12, compared to PCN-12', can be ascribed to both the formation of cuboctahedral cages and the alignment of open metal sites within each cage of the open copper sites in PCN-12, strengthening the H_2-framework interaction. To our knowledge, PCN-12 possesses the highest hydrogen uptake reported for a MOF at 1 bar and 77 K. As polymorphs of each other, PCN-12 and PCN-12' have not only the same formula after solvate removal but also the same atom-to-atom connectivity. However, the gravimetric hydrogen uptake of PCN-12 is 27% higher than that of PCN-12' at 77 K and 1 bar. The reason behind these remarkable improvements can mainly be attributed to the “close packing” strategy, namely, the formation of cuboctahedral cages and the unique alignment of open metal sites in each cuboctahedral cage in PCN-12.

This strategy may have general implications in the search for a practical adsorptive hydrogen-storage material for fuel-cell-driven cars.

MOFs with “close-packing” alignment of open metal sites can increase the number of nearest neighboring open metal sites of each H_2-hosting void in a three-dimensional (3-D) framework so that they can interact directly with the guests (H_2 molecules) inside the void.

(7) Studied the impact of pore size on H_2 storage capacity in MOFs.

The assembly of dicopper paddlewheel SBU and the tetracarboxylate ligand, 5,5'-(1,2-ethynediyl)bis(1,3-benzenedicarboxylate) (ebdc) gave rise to two isomeric NbO-type structures, named PCN-16 and PCN-16'. (Figure 7 Top Scheme)

To check the permanent porosities of the pair of isomers, N_2 sorption isotherms at 77 K were collected for the dehydrated samples. As shown in Figure 7, both PCN-16 and PCN-16' display typical Type-I sorption behaviour. PCN-16 has a BET surface area of 2273 m^2/g (Langmuir surface area, 2800 m^2/g) and a total pore volume of 1.06 cm^3/g while PCN-16' possesses a 1760 m^2/g BET surface area (Langmuir surface area, 2200 m^2/g) and a 0.84 cm^3/g pore volume. The differing pore structures as evidenced by the BET surface areas directly impact the sorption capacities for hydrogen as indicated in Figure 7, PCN-16 demonstrates significantly higher hydrogen adsorption capacity than PCN-16'. At 77 K and 760 torr, PCN-16 can adsorb 2.6 wt% hydrogen, comparable to the values observed in other α phase NbO-type copper MOFs. In contrast, PCN-16' can only adsorb 1.7 wt% hydrogen, much lower than that in PCN-16. This difference persists at higher pressures where the excess hydrogen uptake of PCN-16 saturates at 5.1 wt%, while the saturation for PCN-16' occurs with the value of only 2.9 wt%. Because PCN-16 and PCN-16' are isomers of each other and both crystallize in the same space group and contain similar nanoscopic cages, the superior gas adsorption properties of PCN-16 can mainly be attributed to the pore size, which is smaller than that of PCN-16'.

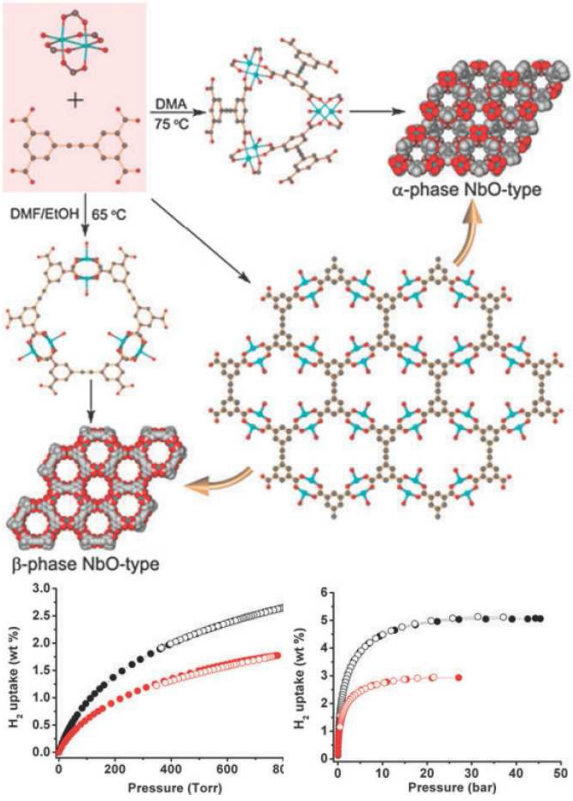

Figure 7. Top Scheme: The formation of the two symmetry-preserving NbO-type phases. Bottom: low-pressure H_2 at 77 K high-pressure H_2 at 77 K; the values are reported as excess adsorption.

The small pores lead to an increased effective surface area, offering more adsorption sites for hydrogen. Indeed, the saturation uptake of hydrogen at 77 K for each isomer is consistent with the different BET surface areas, as explained in a recent analysis. The results above also suggest that α phase NbO-type copper MOFs should be better for gas storage than their β phase counterparts.

(8) Incorporated polyyne unit into MOFs, which has higher H_2 affinity.

A NbO-type metal–organic framework, PCN-46, was constructed based on a polyyne-coupled di-isophthalate linker formed *in situ*. Its permanent porosity was confirmed by both N_2 (77 K) and Ar (77 and 87 K) sorption isotherms. The isotherms show type-I sorption behavior, which is typical for microporous materials. Based on the N_2 sorption isotherm, PCN-46 has a BET surface area of 2500 m^2/g (Langmuir surface area: 2800 m^2/g) and a total pore volume of 1.012 cm^3/g. It has a uniform pore size around 6.8 Å based on the Horvath–Kawazoe model in the Micromeritics ASAP2020 software package (assuming cylinder pore geometry). The high porosity and stable framework make PCN-46 a good candidate for gas storage. At 77 K and 760 Torr, PCN-46 can reversibly adsorb 1.95 wt% of H_2 (Figure 8). Under high pressure range, the saturated excess gravimetric H_2 uptake is 5.31 wt% (56.1 mg/g) at 32 bar. Taking the gaseous H_2 compressed within the void pore at 77 K into

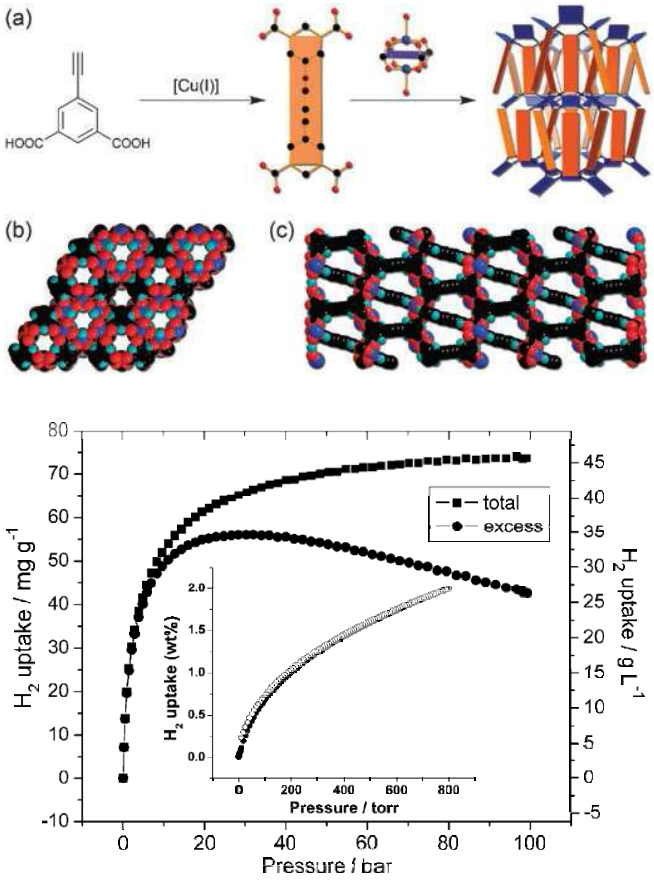

Figure 8. (a) *In situ* formed ligand and the formation of NbO-type framework; (b) atomic packing of PCN-46, viewed through [0 0 1] direction; (c) atomic packing of PCN-46, viewed through [1 0 0] direction. Bottom: Gravimetric and volumetric H_2 uptake in PCN-46 at 77 K (solid symbols, adsorption; open symbols, desorption).

consideration, the total gravimetric H_2 uptake can reach as high as 6.88 wt% (73.9 mg/g) at 97 bar. Calculated from the crystal density of the activated form (0.6185 g/cm^3), PCN-46 has an excess volumetric H_2 uptake of 34.7 g/L (32 bar) and a total volumetric uptake of 45.7 g/L (97 bar). Theoretical studies reveal that given the same MOF structural type, the longer the ligand, the higher the specific surface area, and accordingly the higher the gravimetric H_2 uptake would be. This is further confirmed by the comparison of PCN-46 and other NbO-type MOFs.

The H_2 isosteric adsorption enthalpy of PCN-46 reaches 7.20 kJ/mol at low coverage, and decreased to 4.06 kJ/mol at medium coverage. The increased heat of hydrogen adsorption in PCN-46, compared to those of other NbO type MOFs, can be attributed to the interaction between H_2 molecules and the exposed and delocalized p electrons in the polyyne unit, which is evidently stronger than that for the phenyl rings. A strong interaction between acetylene and a NbO-type MOF containing alkyne unit was also discovered, in which the high hydrogen affinity towards the framework was particularly attributed to the p–p interaction. In addition, the replacement of phenyl rings by polyyne chain leads to a boost of pore volume and hydrogen uptake.

(9) Tuned the pore structure by introducing difference functional groups into MOFs to study the effect on H_2 uptake.

We worked on the synthesis and properties of functional MOFs by rationally designing functionalized ligands. As we all know, MOF-177 is a porous material with high surface area (Langmuir: 5640 m^2/g) and record hydrogen storage (7.0 wt % at 60 bar and 77 K). Our tactics for preparing the functionalized MOF is to construct isostructural MOF-177 by designing a series of new functional

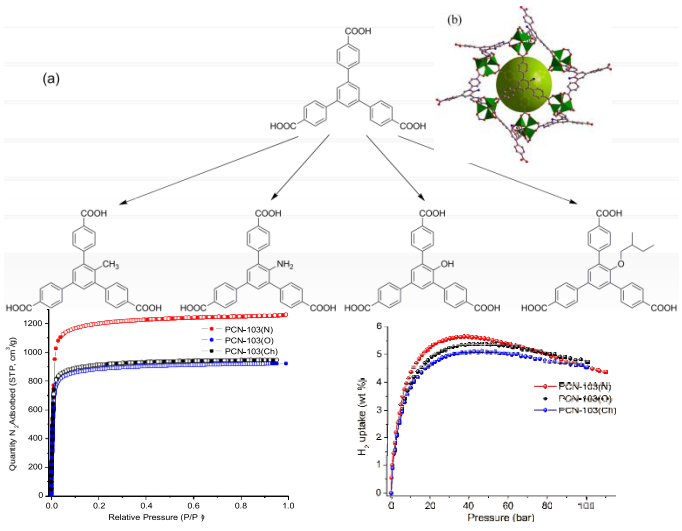

Figure 9. (a)The structure of modified BTB ligands; (b) the crystal structures of PCN-103(C, N, O and Ch) with an approximately spherical pore of 17 Å diameter; bottom left: N_2 sorption isotherms of PCN-103(N, O, Ch) at low pressure; bottom right: H_2 uptakes of PCN-103 at high pressure.

organic ligands with the methyl, amino, hydroxyl and chiral group (Figure 9). As expected, the four new ligands reacted with zinc salt to form four novel MOFs with isostructural MOF-177. Based on the N_2 sorption isotherm, PCN-103(N) has a BET surface area of 4300 m^2/g^{-1} (Langmuir surface area: 5500 m^2/g) and a total pore volume of 1.95 cm^3 g^{-1}, which is similar to those results of MOF-177. PCN-103(O) has a BET surface area of 2866 m^2/g (Langmuir surface area: 4587 m^2/g), while PCN-103(Ch) a BET surface area of 2850 m^2/g (Langmuir surface area: 4144 m^2/g) (Figure 9). The saturated excess gravimetric H_2 uptake of PCN-103(N) is 5.62 wt % at 40 bar, while PCN-103(Ch) has a saturated excess gravimetric H_2 uptake of 5.10 wt % at 43 bar.
In conclusion, the functional groups exert a weak influence to H_2 uptake, The $–NH_2$ and –OH groups can be used as anchors for additional metal ions.

(10) Construct stable and high-surface-area Zr-MOFs, study the effect on gas uptake by introducing different metals into their porphrin linkers.

Solvothermal reactions of metalloporphyrin M-TCPP (TCPP = tetrakis(4-carboxyphenyl)porphyrin, M = Fe, Mn, Co, Ni, Cu, Zn, H_2), $ZrCl_4$ and benzoic acid yielded needle shaped single crystals of PCN-223. Different from the well-known 12-connected Zr_6 cluster observed in the UiO-series of MOFs, only eight edges of the Zr_6 octahedron are bridged by carboxylates from TCPP ligands in PCN-223, while the remaining positions are occupied by terminal OH groups (Figure 10a).
The porosity of PCN-223 has been examined by N_2 adsorption experiments at 77 K. The typical type IV isotherm of PCN-223(Fe) exhibits a steep increase at the point of P/P0 = 0.3, suggesting meso-porosity. A N_2 uptake of 1,009 cm^3/g and a BET surface area of 2,200 m^2/g have been observed for PCN-223(Fe), the pore volume of 1.56 cm^3/g is also in good agreement with the calculated pore volume of 1.63 cm^3/g. Other PCN-223 MOFs with different porphyrin centers also displayed similar type IV N_2 sorption isotherms and gave surface area, N_2 uptake, and total pore volume up to 2,312 m^2/g, 1,067 cm^3/g, and 1.65 cm^3/g, respectively.

The PXRD patterns remain intact upon immersion in water, boiling water, as well as 2M, 4M, 8M, and even concentrated HCl aqueous solutions for 24 h, suggesting no phase transition or framework collapse happening during these treatments (Figure 10b). More importantly, the N_2 sorption isotherms remained almost the same upon all treatments, which further confirmed the intactness of the tested frameworks. Strikingly, PCN-223(Fe) survived even after the treatment with concentrated HCl, a strong acid, which has rarely been observed for MOF materials, showing its exceptionally high chemical stability.

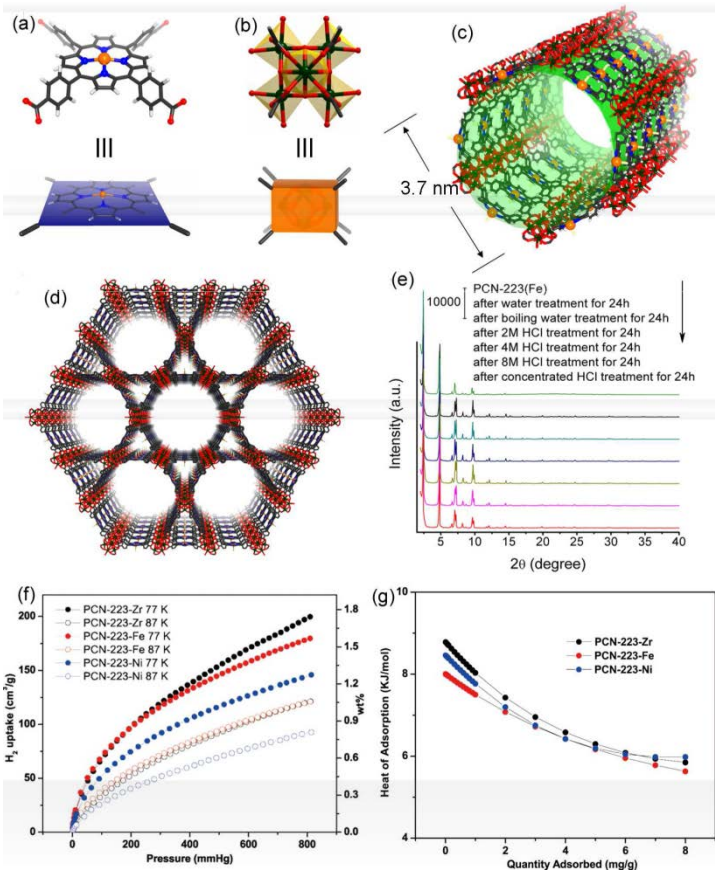

Figure 10. (a) The metalloporphyrin ligand Fe-TCPP. (b) 8-connected Zr_6 clusters (light orange cuboid). (c) 3-D network in Kagome-like topology with 1-D large channels. (d) Crystal structure and underlying network topology of PCN-223(Fe). (e) Powder X-ray diffraction pattern upon treatments with water, boiling water, 2 M, 4 M, 8 M and even concentrated HCl. (f) Low pressure hydrogen isotherms of PCN-223 at 77 and 87 K. (g) Calculated heats of adsorption of PCN-223.

Variable-temperature measurements reveal isosteric heats of adsorption of 8.7, 8.0, and 8.5 kJ/mol for PCN-223(Zr), PCN-223(Fe), and PCN-223(Ni), respectively, at zero loading (Figure 10g). The high value can be partial attributed to the incorporated metal centers in the prophyrin ligand.

(11) Design and synthesize PPNs with high chemical stability suitable for further decoration.

Conventional Yamamoto homo-coupling reaction for polymerization was carried out at 80 ℃ with DMF as the solvent. However, when the sa me reaction condition was applied to tetrakis(4-bromophenyl)silane or tetrakis(4-bromophenyl)admantane, the surface

areas of the synthesized materials were much lower than the calculated data. With the assumption that reduced temperature would slow down the reaction to yield polymers with higher molecular weight and avoid any unwanted side reactions, we adopted an optimized Yamamoto homo-coupling procedure, in which the reactions were carried out at room temperature in a DMF/THF mixed solvent. Using this procedure, we were able to synthesize PPN-3, PPN-4, and PPN-5 with exceptionally high surface areas (Figure 11a and 11b). The surface area of PPN-3 synthesized through this procedure is much higher than the value previously reported, and the surface area of PPN-4 is close to the value predicted based on the molecular model, indicating the excellence of this optimized procedure. With the BET surface area of 6461 m^2/g and Langmuir surface area of 10063 m^2/g, PPN-4 possesses, to the best of our knowledge, one of the highest surface area among all the reported porous materials so far. In addition, most of the pores in PPN-4 sit within the range of microporous or microporous/mesoporous range, which serves remarkably for gas storage purposes.

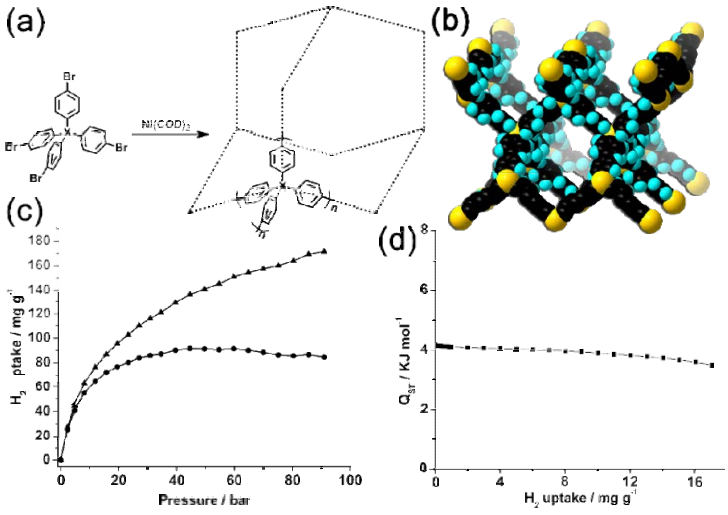

Figure 11. (a) Synthetic route for PPN-3 (X: Adamantane), PPN-4 (X: Si), PPN-5 (X: Ge), and PAF-1 (X: C); (b) The default noninterpenetrated diamondoid network of PPN-4 (black, C; cyan, H; yellow, Si); (c) Excess and total H_2 adsorption isotherms of PPN-4 at 77 K; (d) Isosteric heat of adsorption for H_2 in PPN-4.

PPNs, PPN-3, PPN-4, and PPN-5 are off-white powders, not soluble in common organic solvents. There is no residual bromine from the elemental analysis result, indicating the completion of the reaction and the efficiency of Yamamoto homo-coupling. Surprisingly, a trace amount of nitrogen was detected in PPN-3 and PPN-5 (0.14 wt% and 0.11 wt%, respectively), which probably comes from the trapped 2,2'-bipyridine within the shrunken pores caused by network interpenetration. This network interpenetration may also accounts for the reduced experimental surface areas of PPN-3 and PPN-5 compared with the calculated data. Thermogravimetric analysis (TGA)

data show the three polymers possess good thermal stability and high decomposition temperatures of more than 450 ℃ in a nitrogen atmo sphere. In addition, PPN-4 retains its structural integrity after being exposed to air for one month, as indicated by virtually no drop of N_2 uptake capacity at 77 K.

The exceptionally high surface area combined with excellent stability make PPN-4 a very attractive candidate for gas storage applications, particularly in H_2 for clean energy purposes. To evaluate its gas storage capacity, high-pressure excess adsorption of H_2 within PPN-4 were measured at 77 K (liquid nitrogen bath). As shown in Figure 11c, the excess H_2 uptake of PPN-4 at 77 K and 55 bar can reach 91 mg/g (8.34 wt%) (total uptake: 158 mg/g, 13.6 wt%, 80 bar), which is by far the highest among all amorphous materials, and is also comparable to the best value reported in MOFs. The isosteric heat of adsorption for H_2 is around 4 kJ mol^{-1} (Figure 11d), which fits within the range of physisorption and indicates that the high surface area might be the sole factor in determining this high H_2 uptake capacity. Unlike MOFs, whose H_2 uptake capacity will decrease after several uptake-release cycles, the H_2 uptake capacity of PPN-4, even being exposed to air for several days, can be simply regenerated by heating under vacuum. The excellent physicochemical stability and impressively high delivery capacity (71 mg/g, 77 K, from 1.5 bar to 55 bar) make PPN-4 the currently unbeatable material for cryogenic H_2 storage application.

(12) Incorporated metal ions into PPNs for enhanced isosteric heats of hydrogen adsorption.

Theoretical studies on MOFs and PPNs materials have suggested that introduction of light, non-transition metal ions such as Li^+, Na^+ or Mg^{2+} might afford non-dissociative hydrogen binding, thus enhancing overall adsorption of H_2. In particular, Li-doped materials appear to be especially interesting in this regard. Here we report the post-grafting of PPN-6 with sulfonic acid and lithium sulfonate. PPN-6 (also known as PAF-1) was synthesized using an optimized Yamamoto homo-coupling reaction of tetrakis(4-bromophenyl)methane. The default diamondoid framework topology imposed by the tetrahedral monomers provides widely open and interconnected pores to efficiently

prevent the formation of “dead space”, more importantly, the extremely robust all-carbon scaffold of the network can stand harsh reaction conditions and makes it perfect to build up polar organic groups on the biphenyl units; indeed, by reacting with chlorosulfonic acid in dichloromethane, PPN-6 was modified into PPN-6-SO_3H, which was further neutralized to produce PPN-6-SO_3Li (Figure 12a). Nitrogen gas adsorption/desorption isotherms of the three networks were collected at 77K (Figure 12b). Notably, the huge hysteresis in PPN-6 adsorption/desorption isotherm disappeared into nearly type-I isotherms in functionalized PPN-6. The BET surface areas were calculated from the adsorption branch of the nitrogen isotherms over a BET-theory-satisfied pressure range and were found to be 4023, 1242, and 1170 m^2/g for PPN-6, PPN-6-SO_3H and PPN-6-SO_3Li respectively. The pore size distributions of the three networks have been calculated with their N_2 adsorption isotherms at 77 K (Figure 12c). Along with the decrease of surface area, the pore size becomes progressively reduced with aromatic sulfonation and lithiation. Recent studies have indicated several features that are desirable for enhancing storage capacity of small gas molecules. One such feature is the suitable pore size commensurate with the size of gas molecule. The relatively small pore sizes of functionalized PPN-6 fall into the range of 5.0-10.0 Å. Though the experimental BET surface of PCN-6-SO3Li area decreased, the H_2 isosteric heat

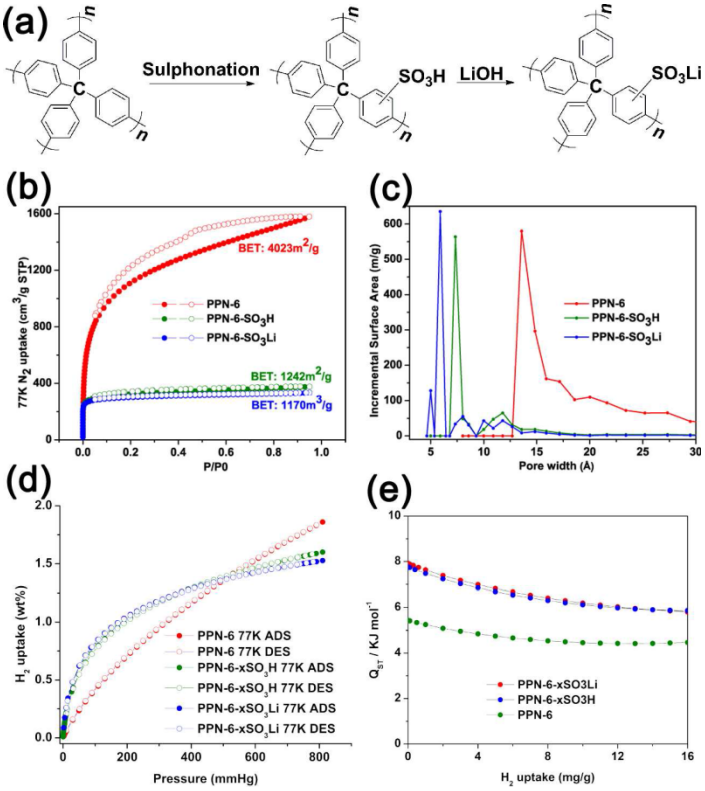

Figure 12. (a) Synthesis and post-synthetic grafting of PPN-6-X; (b) (a) N_2 adsorption (closed)/desorption (open) isotherms of PPN-6-X at 77 K; (c) Pore size distribution curves of PPN-6-X; (d) Excess adsorption isotherms of PPN-6-X at 77 K; (d) Isosteric heat of adsorption for H_2 in PPN-6-X.

increased 47% (Figure 12d and 12e), which is consistent with theoretical calculation. The introduction of other metal will also be studied, such as Mg, Ti, Ni, Co and so on.

(13) Ligand truncation strategy for enhanced H_2 adsorption

Symmetrical linker extension is a general method to synthesize new MOFs that bear the same network topology as the nonextended frameworks, but extended linkers might also result in framework interpenetration or collapse upon activation. The reverse of linker extension is ligand truncation. This proposed strategy provides a method to introduce new types of building blocks with reduced symmetry, and the obtained frameworks might possess new topologies and interesting properties for H_2 adsorption.

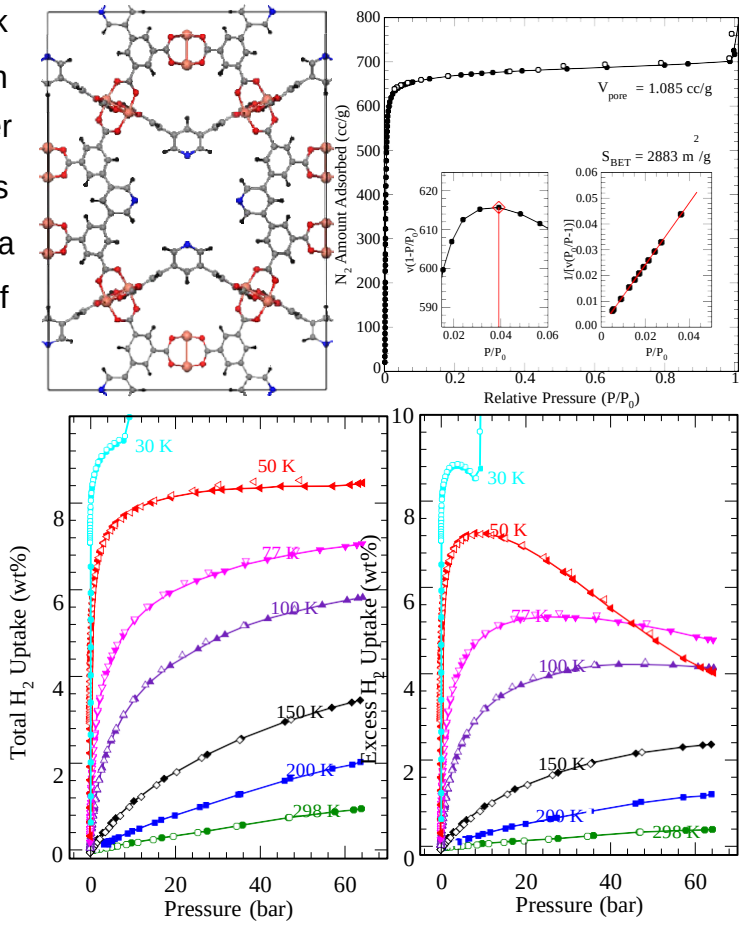

Figure 13. Top left: crystal Structure of PCN-305. Top right: nitrogen isotherm of PCN-305 and BET plot. Bottom left: total H_2 uptake of PCN-305 at different temperatures. Bottom right: excess H_2 uptake of PCN-305 at different temperatures.

A series of C_2 symmetric ligands with different functional groups have been designed and synthesized via Suzuki reaction. Solvothermal reaction between these ligands and $Cu(NO_3)_2 \cdot 2.5H_2O$ in dimethylacetamide (DMA) with tetrafluoroboric acid (HBF_4, 48% w/w aqueous solution) afforded a three-dimensional (3D) framework, designated as PCN-30X. PCN-30X adopt a very rare 4-c 4-nodal net (Figure 13) with topological point symbol of $\{4.6^4.8\}_2\{4^2.6^4\}\{6^4.8^2\}_2\{6^6\}$, which is previously unreported.

H_2 sorption isotherms were collected for the isoreticular MOFs. They exhibited high H_2 uptake capacity at low pressure (1 bar). Among them, PCN-308 with $–CF_3$ functional groups exhibits a hydrogen uptake of 2.67 wt% at 1 bar and 77 K, which is among the highest for MOFs at low pressure.

H_2 high pressure adsorption isotherms were measured for PCN-305, PCN-305 has a BET surface area of 2883 m^2/g, which is well matched with the calculated value by PLATON (3100 m^2/g). On the Figure 13 (top right), we show the nitrogen isotherm for PCN-305. From maximum adsorptions near Po, we get pore volume of 1.085 cm^3/g. On the left inset of Figure 13 (top right), we show the consistency plot which indicates that the BET range P/Po ~ 0.04. On the right inset of Figure 13 (top right), we show the BET plot and the fit, giving a surface area of 2883 m^2/g. The pore volume and surface area are in good agreement with the PLATON calculations.

The total and excess hydrogen isotherms for PCN-305 are shown in Figure 13 (bottom left). The numbers are expected based on the pore volume and surface area of PCN-305. For excess isotherm, at 77 K, usually 500 m^2/g gives 1 wt%, which is the case for PCN-305.

Q_{st} is around 5.2 kJ/mol initially and then start to decrease down to 4 kJ/mol. These numbers are typical for copper-paddle wheel MOFs. The initial flat Q_{st} is a sign that the main adsorption sites are copper sites. For H_2, the H_2-H_2 interaction is very small and therefore we do not see such increase in Q_{st} with increasing gas uptake.

(14) Constructed MOF from a highly conjugated ligand exhibiting a high hydrogen uptake capacity

A new porous metal-organic framework, PCN-20 with a twisted boracite net topology, was constructed based on a highly conjugated planar tricarboxylate ligand.

The N_2 sorption isotherms reveal that PCN-20 exhibits typical type I sorption behavior without hysteresis, a characteristic of microporous materials. Derived from the N_2 adsorption data, the Langmuir surface area of PCN-20 is 4237 m^2/g, corresponding to a Brunauer-Emmett-Teller surface area of 3525 m^2/g and a pore volume of 1.59 cm^3/g. The Langmuir surface area of PCN-20 is much higher than those of Cu-BTC and PCN-

60, confirming the theoretical prediction that fused aromatic rings favor high surface area in porous MOFs.

To evaluate the hydrogen storage performance of PCN-20, hydrogen sorption isotherms were measured at 77 K under both low and high pressures. As shown in Figure 14, PCN-20 can adsorb 2.1 wt % (excess) hydrogen at 1 bar and 77 K. With the pressure increased to 50 bar (Figure 14), its excess gravimetric hydrogen uptake capacity can reach as high as 6.2 wt %, which is among the highest for reported porous MOFs. This value is much higher than those of Cu-BTC (3.4 wt %) and PCN-60 (4.0 wt %) under the same conditions and can be ascribed to its much larger surface area, resulting from the highly conjugated fused triphenylene ring.

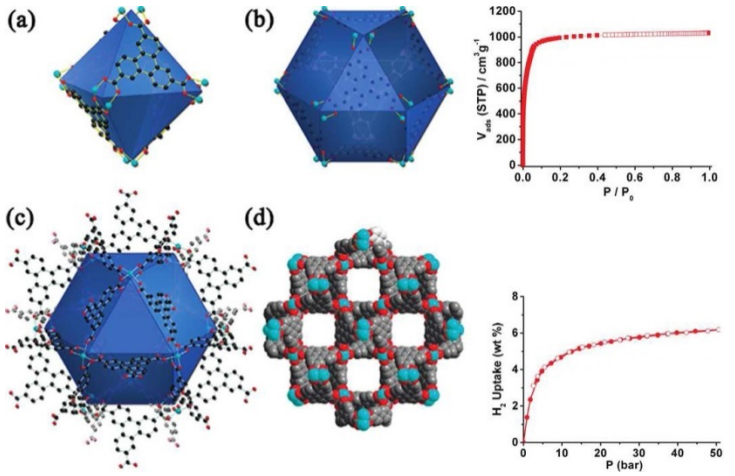

Figure 14. (a) Octahedral cage in PCN-20. (b) Cuboctahedral cage with alignment of the unsaturated metal centers (UMCs) in PCN-20. (c) Cuboctahedral cage with open metal sites aligned orthogonally in PCN-20. (d) Square channels viewed from the [0 0 1] direction (hydrogen atoms were omitted for clarity). Top right: nitrogen sorption isotherms for PCN-20. Bottom right: high pressure H_2 sorption isotherms of PCN-20 at 77 K.

(15) Built up porous lanthanide MOFs and studied their potential application in gas adsorption.

Compared to first-row transition metals, lanthanides have larger coordination spheres and more flexible coordination geometries. So far, research for reported lanthanide MOFs has been focused on magnetic and photoluminescent properties; however, the construction of porous lanthanide MOFs and their potential application in gas adsorption have been much less developed. We have recently extended the application of the TATB ligand for the construction of lanthanide MOFs with novel architectures and interesting properties. Under solvothermal conditions, the reactions of the TATB ligand with $Dy(NO_3)_3$, $Er(NO_3)_3$, $Y(NO_3)_3$, and $Yb(NO_3)_3$ afforded four isostructual microporous lanthanide MOFs, designated as PCN-17 (Dy), PCN-17 (Er), PCN-17 (Y) and PCN-17 (Yb), respectively.

The four MOFs all adopt the square-planar $Ln_4(\mu4\text{-}H_2O)$ SBU (Ln = Dy, Er, Y and Yb), with the $\mu4\text{-}H_2O$ residing at the center of the square of four Ln atoms. In all of the four structures, every TATB ligand links three $Ln_4(\mu4\text{-}H_2O)$ SBUs, every $Ln_4(\mu4\text{-}H_2O)$ SBU connects eight trigonal-planar TATB ligands and four sulfate ligands to form an infinite framework. There exist two types of cages in their structures: one is a truncated octaheral cage defined by six $Ln_4(\mu4\text{-}H_2O)$ SBUs at the corners and eight TATB ligands on the faces, and the other one is a cuboctahedral cage enclosed by eight truncated octahedral cages occupying the vertices of the cube. Every cuboctahedral cage connects eight truncated octahedral cages via facesharing, and each truncated octahedral cage links six cuboctahedral cages to form a (8,3)-net framework. Two such (8,3)-nets are mutually interpenetrated because of the π-π interactions of the TATB ligand pairs as reflected in the short distance between the centers of the two triazine rings of the TATB ligand pairs. The staggered TATB ligand pairs resulting from strong π-π interactions lead to the truncated octahedral cages of one set framework enclosed by the cuboctahedral cages of the other set framework with the triangular face-sharing. This closes the windows of the truncated octahedral cages and also reduces the size of the opening of the cuboctahedral cages, which is further restricted by the bridging sulfate ligands. Overall, their structures can be described as sulfate-bridged doubly interpenetrated (8,3)-connected nets. The removal of the $\mu4\text{-}H_2O$ in the $Ln4(\mu4\text{-}H_2O)$ SBUs can result in some openings of ~3.5 Å.

To test their permanent porosities, CO_2 adsorption studies were performed utilizing fully activated samples. CO_2 adsorption isotherms of the four fully activated MOFs reveals typical type-I behaviors as expected for microporous materials. Fittings of the BET equation to the adsorption isotherms of CO_2 give the estimated surface areas of 738 m^2/g, 606 m^2/g, 814 m^2/g, and 820 m^2/g for PCN-17 (Dy), PCN-17 (Er), PCN-17 (Y), and PCN-17 (Yb), respectively. Using the Dubinin-Radushkevich equation, the pore volumes of PCN-17 (Dy), PCN-17 (Er), PCN-17 (Y), and PCN-17 (Yb) are estimated to be 0.31 cm^3/g, 0.25 cm^3/g, 0.33 cm^3/g, and 0.34 cm^3/g, respectively. Low-pressure H_2 sorption measurements of these compounds were also performed. All of the four porous MOFs can adsorb a moderate amount of H_2 (110 cm^3/g for PCN-17 (Dy), 90 cm^3/g for PCN-17 (Er), 123 cm^3/g for PCN-17 (Y), and 105 cm^3/g for PCN-17 (Yb)) with typical

type-I behaviors. However, the amounts of CO adsorbed by the four MOFs are very limited, and the selectivity of H_2 over CO is 3.6, 1.9, 1.5, and 1.7 for PCN-17 (Yb), PCN-17 (Dy), PCN-17 (Er), and PCN-17 (Y), respectively. The selective adsorption of H_2 over CO exhibited by these porous lanthanide MOFs promises its potential applications in the separation of hydrogen from carbon monoxide in fuel cell applications.

5. Conclusions and Future Directions

We have achieved:

- High Surface Area: A library with over 100 ligands have been created, more than 30 porous materials with over 2000 m^2/g accessible surface area have been synthesized and their hydrogen storage have been measured.

- High Gravimetric Capacity: The excess H_2 uptake of PPN-4 at 77 K and 55 bar can reach 91 mg/g (8.34 wt%) (total uptake: 158 mg/g, 13.6 wt%, 80 bar); the delivery capacity of PPN-4 can reach 71 mg/g at 77 K (from 1.5 bar to 55 bar); the excess hydrogen uptake of PPN-4 was 1.17 wt% at 295 K and 90 bar.

- High Volumetric Capacity: The excess H_2 uptake of PCN-12 at 77 K and 50 bar can reach 45.7 g/L; the excess H_2 uptake of PCN-6 at 77 K and 50 bar can reach 40.2 g/L; the maximum volumetric hydrogen adsorption of PPN-4 is 28 g/L at 77 K and 90 bar, due to its exceptionally high thermal and chemical stability, PPN-4 demonstrated that it could be compressed to half its size without losing its porosity, thus, the volumetric uptake of H_2 would be doubled by compression (28.0 g/L × 2 = 56.0 g/L at 77K and 90 bar).

- Optimized Pore Size: We experimentally established the optimum pore size for maximum hydrogen storage. For example, catenation was utilized to reduce pore sizes in porous MOFs to improve the hydrogen uptake of MOFs.

- Enhanced Binding Energy: Well-defined hydrogen occupation sites and their alignment are critical for the high hydrogen binding energy. For example, the hydrogen adsorption heat of PCN-12 can reach as high as 12.5 kJ/mol at low

coverage because of the optimization of the alignment of the coordinatively unsaturated metal centers.

Future Directions:

Two of the key factors limiting the hydrogen uptake of MOFs and PPNs are the restricted surface area and the weak interaction between hydrogen and the framework. We will continue to explore the metal-doped MOFs and PPNs with high surface area, especially, the high electron affinity of the sp^2 and sp carbon framework in the PPNs can essentially separate the charge from the metal center, thus providing strong stabilization of the H_2 and improving the hydrogen uptake. The goal is to increase the heat of hydrogen adsorption, gravimetric excess capacities and volumetric excess capacities at the same time.

- High throughput screening by using robotic system in the synthesis of MOFs with ligands in library.
- Further enhancement of H_2-MOF interaction by incorporating coordinatively unsaturated metal centers (heat of adsorption 15 kJ mol^{-1}). Main group metals such as Li, Mg and Ca and multivalent metals, such as V^{3+}, Fe^{3+},Ti^{3+}, etc. will be tested.
- Incorporating different metal cations (such as Fe^{2+}) into porphyrin center of Zr-MOFs, and performing elastic diffuse neutron-scattering studies to demonstrate multiple H_2 per open metal site in MOFs.

6. Publications

1. Hydrogen storage in metal-organic frameworks. Collins, D. J.; Zhou, H.-C., *Journal Of Materials Chemistry* **2007,** *17* (30), 3154-3160.

2. Rationally Designed Micropores within a Metal−Organic Framework for Selective Sorption of Gas Molecules. Chen, B.; Ma, S.; Zapata, F.; Fronczek, F. R.; Lobkovsky, E. B.; Zhou, H.-C., *Inorganic Chemistry* **2007,** *46* (4), 1233-1236.

3. Framework-Catenation Isomerism in Metal−Organic Frameworks and Its Impact on Hydrogen Uptake. Ma, S.; Sun, D.; Ambrogio, M.; Fillinger, J. A.; Parkin, S.; Zhou, H.-C., *Journal Of The American Chemical Society* **2007,** *129* (7), 1858-1859.

4. A Mesh-Adjustable Molecular Sieve for General Use in Gas Separation. Ma, S.; Sun, D.; Wang, X.-S.; Zhou, H.-C., *Angewandte Chemie International Edition* **2007,** *46* (14), 2458-2462.

5. Construction of Robust Open Metal−Organic Frameworks with Chiral Channels and Permanent Porosity. Sun, D.; Ke, Y.; Collins, D. J.; Lorigan, G. A.; Zhou, H.-C., *Inorganic Chemistry* **2007,** *46* (7), 2725-2734.

6. Metal−Organic Framework Based on a Trinickel Secondary Building Unit Exhibiting Gas-Sorption Hysteresis. Ma, S.; Wang, X.-S.; Manis, E. S.; Collier, C. D.; Zhou, H.-C., *Inorganic Chemistry* **2007,** *46* (9), 3432-3434.

7. A Triply Interpenetrated Microporous Metal−Organic Framework for Selective Sorption of Gas Molecules. Chen, B.; Ma, S.; Hurtado, E. J.; Lobkovsky, E. B.; Zhou, H.-C., *Inorganic Chemistry* **2007,** *46* (21), 8490-8492.

8. Ultramicroporous Metal−Organic Framework Based on 9,10-Anthracenedicarboxylate for Selective Gas Adsorption. Ma, S.; Wang, X.-S.; Collier, C. D.; Manis, E. S.; Zhou, H.-C., *Inorganic Chemistry* **2007,** *46* (21), 8499-8501.

9. Metal-Organic Framework from an Anthracene Derivative Containing Nanoscopic Cages Exhibiting High Methane Uptake. Ma, S.; Sun, D.; Simmons, J. M.; Collier, C. D.; Yuan, D.; Zhou, H.-C., *Journal Of The American Chemical Society* **2008,** *130* (3), 1012-1016.

10. Nano/Microporous Materials: Hydrogen-Storage Materials. In *Encyclopedia of Inorganic Chemistry*, Collins, D. J.; Zhou, H.-C., John Wiley & Sons, Ltd: **2006**.

11. Metal−Organic Frameworks Based on Double-Bond-Coupled Di-Isophthalate Linkers with High Hydrogen and Methane Uptakes. Wang, X.-S.; Ma, S.; Rauch, K.; Simmons, J. M.; Yuan, D.; Wang, X.; Yildirim, T.; Cole, W. C.; López, J. J.; Meijere, A. d.; Zhou, H.-C., *Chemistry Of Materials* **2008,** *20* (9), 3145-3152.

12. A Coordinatively Linked Yb Metal–Organic Framework Demonstrates High Thermal Stability and Uncommon Gas-Adsorption Selectivity. Ma, S.; Wang, X.-S.; Yuan, D.; Zhou, H.-C., *Angewandte Chemie International Edition* **2008,** *47* (22), 4130-4133.

13. The current status of hydrogen storage in metal-organic frameworks. Zhao, D.; Yuan, D.; Zhou, H.-C., *Energy & Environmental Science* **2008,** *1* (2), 222-235.

14. Enhancing H2 Uptake by “Close-Packing” Alignment of Open Copper Sites in Metal–Organic Frameworks. Wang, X.-S.; Ma, S.; Forster, P. M.; Yuan, D.; Eckert, J.; López, J. J.; Murphy, B. J.; Parise, J. B.; Zhou, H.-C., *Angewandte Chemie International Edition* **2008,** *47* (38), 7263-7266.

15. Further Investigation of the Effect of Framework Catenation on Hydrogen Uptake in Metal−Organic Frameworks. Ma, S.; Eckert, J.; Forster, P. M.; Yoon, J. W.; Hwang, Y. K.; Chang, J.-S.; Collier, C. D.; Parise, J. B.; Zhou, H.-C., *Journal Of The American Chemical Society* **2008,** *130* (47), 15896-15902.

16. Microporous Lanthanide Metal-Organic Frameworks Containing Coordinatively Linked Interpenetration: Syntheses, Gas Adsorption Studies, Thermal Stability Analysis, and Photoluminescence Investigation. Ma, S.; Yuan, D.; Wang, X.-S.; Zhou, H.-C., *Inorganic Chemistry* **2009,** *48* (5), 2072-2077.

17. Selective gas adsorption and separation in metal-organic frameworks. Li, J.-R.; Kuppler, R. J.; Zhou, H.-C., *Chemical Society Reviews* **2009,** *38* (5), 1477-1504.

18. Interconversion between Molecular Polyhedra and Metal−Organic Frameworks. Li, J.-R.; Timmons, D. J.; Zhou, H.-C., *Journal Of The American Chemical Society* **2009,** *131* (18), 6368-6369.

19. Preparation and Gas Adsorption Studies of Three Mesh-Adjustable Molecular Sieves with a Common Structure. Ma, S.; Sun, D.; Yuan, D.; Wang, X.-S.; Zhou, H.-C., *Journal Of The American Chemical Society* **2009,** *131* (18), 6445-6451.

20. A Three-Dimensional Porous Metal−Organic Framework Constructed from Two-Dimensional Sheets via Interdigitation Exhibiting Dynamic Features. Ma, S.; Sun, D.; Forster, P. M.; Yuan, D.; Zhuang, W.; Chen, Y.-S.; Parise, J. B.; Zhou, H.-C., *Inorganic Chemistry* **2009,** *48* (11), 4616-4618.

21. Design and Construction of Metal–Organic Frameworks for Hydrogen Storage and Selective Gas Adsorption. In *Design and Construction of Coordination Polymers*, Ma, S.-Q.; Collier, C. D.; Zhou, H.-C., John Wiley & Sons, Inc.: **2009**; 353-373.

22. Investigation of Gas Adsorption Performances and H2 Affinities of Porous Metal-Organic Frameworks with Different Entatic Metal Centers. Ma, S.; Yuan, D.; Chang, J.-S.; Zhou, H.-C., *Inorganic Chemistry* **2009,** *48* (12), 5398-5402.

23. A nanotubular metal-organic framework with permanent porosity: structure analysis and gas sorption studies. Ma, S.; Simmons, J. M.; Yuan, D.; Li, J.-R.; Weng, W.; Liu, D.-J.; Zhou, H.-C., *Chemical Communications* **2009,** (27), 4049-4051.

24. Stabilization of Metal−Organic Frameworks with High Surface Areas by the Incorporation of Mesocavities with Microwindows. Zhao, D.; Yuan, D.; Sun, D.; Zhou, H.-C., *Journal Of The American Chemical Society* **2009,** *131* (26), 9186-9188.

25. Potential applications of metal-organic frameworks. Kuppler, R. J.; Timmons, D. J.; Fang, Q.-R.; Li, J.-R.; Makal, T. A.; Young, M. D.; Yuan, D.; Zhao, D.; Zhuang, W.; Zhou, H.-C., *Coordination Chemistry Reviews* **2009,** *253* (23–24), 3042-3066.

26. A Large-Surface-Area Boracite-Network-Topology Porous MOF Constructed from a Conjugated Ligand Exhibiting a High Hydrogen Uptake Capacity. Wang, X.-S.; Ma, S.; Yuan, D.; Yoon, J. W.; Hwang, Y. K.; Chang, J.-S.; Wang, X.; Jørgensen, M. R.; Chen, Y.-S.; Zhou, H.-C., *Inorganic Chemistry* **2009,** *48* (16), 7519-7521.

27. Metal–Organic Hendecahedra Assembled from Dinuclear Paddlewheel Nodes and Mixtures of Ditopic Linkers with 120 and 90°Bend Angles. Li, J .-R.; Zhou, H.-C., *Angewandte Chemie International Edition* **2009,** *48* (45), 8465-8468.

28. Gas storage in porous metal-organic frameworks for clean energy applications. Ma, S.; Zhou, H.-C., *Chemical Communications* **2010,** *46* (1), 44-53.

29. An unusual case of symmetry-preserving isomerism. Sun, D.; Ma, S.; Simmons, J. M.; Li, J.-R.; Yuan, D.; Zhou, H.-C., *Chemical Communications* **2010,** *46* (8), 1329-1331.

30. Metal–Organic Frameworks with Exceptionally High Methane Uptake: Where and How is Methane Stored? Wu, H.; Simmons, J. M.; Liu, Y.; Brown, C. M.; Wang, X.-S.; Ma, S.; Peterson, V. K.; Southon, P.

D.; Kepert, C. J.; Zhou, H.-C.; Yildirim, T.; Zhou, W., *Chemistry – A European Journal* **2010,** *16* (17), 5205-5214.

31. Hydrogen and Methane Storage in Metal-Organic Frameworks. In *Metal-Organic Frameworks*, Collins, D. J.; Ma, S.; Zhou, H.-C., John Wiley & Sons, Inc.: **2010**; 249-266.

32. A NbO-type metal-organic framework derived from a polyyne-coupled di-isophthalate linker formed in situ. Zhao, D.; Yuan, D.; Yakovenko, A.; Zhou, H.-C., *Chemical Communications* **2010,** *46* (23), 4196-4198.

33. An Isoreticular Series of Metal–Organic Frameworks with Dendritic Hexacarboxylate Ligands and Exceptionally High Gas-Uptake Capacity. Yuan, D.; Zhao, D.; Sun, D.; Zhou, H.-C., *Angewandte Chemie International Edition* **2010,** *49* (31), 5357-5361.

34. Introduction of cavities up to 4 nm into a hierarchically-assembled metal-organic framework using an angular, tetratopic ligand. Zhuang, W.; Ma, S.; Wang, X.-S.; Yuan, D.; Li, J.-R.; Zhao, D.; Zhou, H.-C., *Chemical Communications* **2010,** *46* (29), 5223-5225.

35. Bridging-ligand-substitution strategy for the preparation of metal–organic polyhedra. Li, J.-R.; Zhou, H.-C., *Nat Chem* **2010,** *2* (10), 893-898.

36. Porous Polymer Networks: Synthesis, Porosity, and Applications in Gas Storage/Separation. Lu, W.; Yuan, D.; Zhao, D.; Schilling, C. I.; Plietzsch, O.; Muller, T.; Bräse, S.; Guenther, J.; Blümel, J.; Krishna, R.; Li, Z.; Zhou, H.-C., *Chemistry Of Materials* **2010,** *22* (21), 5964-5972.

37. Tuning the Topology and Functionality of Metal−Organic Frameworks by Ligand Design. Zhao, D.; Timmons, D. J.; Yuan, D.; Zhou, H.-C., *Accounts Of Chemical Research* **2011,** *44* (2), 123-133.

38. Ligand Bridging-Angle-Driven Assembly of Molecular Architectures Based on Quadruply Bonded Mo−Mo Dimers. Li, J.-R.; Yakovenko, A. A.; Lu, W.; Timmons, D. J.; Zhuang, W.; Yuan, D.; Zhou, H.-C., *Journal Of The American Chemical Society* **2010,** *132* (49), 17599-17610.

39. Functional Mesoporous Metal−Organic Frameworks for the Capture of Heavy Metal Ions and Size-Selective Catalysis. Fang, Q.-R.; Yuan, D.-Q.; Sculley, J.; Li, J.-R.; Han, Z.-B.; Zhou, H.-C., *Inorganic Chemistry* **2010,** *49* (24), 11637-11642.

40. Surface functionalization of metal-organic polyhedron for homogeneous cyclopropanation catalysis. Lu, W.; Yuan, D.; Yakovenko, A.; Zhou, H.-C., *Chemical Communications* **2011,** *47* (17), 4968-4970.

41. Isomerism in Metal–Organic Frameworks: “Framework Isomers”. Makal, T. A.; Yakovenko, A. A.; Zhou, H.-C., *The Journal of Physical Chemistry Letters* **2011,** *2* (14), 1682-1689.

42. Pressure-Responsive Curvature Change of a “Rigid” Geodesic Ligand in a (3,24)-Connected Mesoporous Metal–Organic Framework. Yuan, D.; Zhao, D.; Zhou, H.-C., *Inorganic Chemistry* **2011,** *50* (21), 10528-10530.

43. Robust Metal–Organic Framework with An Octatopic Ligand for Gas Adsorption and Separation: Combined Characterization by Experiments and Molecular Simulation. Zhuang, W.; Yuan, D.; Liu, D.; Zhong, C.; Li, J.-R.; Zhou, H.-C., *Chemistry Of Materials* **2011,** *24* (1), 18-25.

44. Sulfonate-Grafted Porous Polymer Networks for Preferential CO2 Adsorption at Low Pressure. Lu, W.; Yuan, D.; Sculley, J.; Zhao, D.; Krishna, R.; Zhou, H.-C., *Journal Of The American Chemical Society* **2011,** *133* (45), 18126-18129.

45. The current status of hydrogen storage in metal-organic frameworks-updated. Sculley, J.; Yuan, D.; Zhou, H.-C., *Energy & Environmental Science* **2011,** *4* (8), 2721-2735.

46. A porous metal-organic framework with helical chain building units exhibiting facile transition from micro- to meso-porosity. Park, J.; Li, J.-R.; Carolina Sanudo, E.; Yuan, D.; Zhou, H.-C., *Chemical Communications* **2012,** *48* (6), 883-885.

47. A novel MOF with mesoporous cages for kinetic trapping of hydrogen. Fang, Q.-R.; Yuan, D.-Q.; Sculley, J.; Lu, W.-G.; Zhou, H.-C., *Chemical Communications* **2012,** *48* (2), 254-256.

48. Stepwise adsorption in a mesoporous metal-organic framework: experimental and computational analysis. Yuan, D.; Getman, R. B.; Wei, Z.; Snurr, R. Q.; Zhou, H.-C., *Chemical Communications* **2012,** *48* (27), 3297-3299.

49. A Highly Porous and Robust (3,3,4)-Connected Metal–Organic Framework Assembled with a 90° Bridging-Angle Embedded Octacarboxylate Ligand. Lu, W.; Yuan, D.; Makal, T. A.; Li, J.-R.; Zhou, H.-C., *Angewandte Chemie International Edition* **2012,** *51* (7), 1580-1584.

50. Highly Potent Bactericidal Activity of Porous Metal-Organic Frameworks. Zhuang, W.; Yuan, D.; Li, J.-R.; Luo, Z.; Zhou, H.-C.; Bashir, S.; Liu, J., *Advanced Healthcare Materials* **2012,** *1* (2), 225-238.

51. A versatile metal-organic framework for carbon dioxide capture and cooperative catalysis. Park, J.; Li, J.-R.; Chen, Y.-P.; Yu, J.; Yakovenko, A. A.; Wang, Z. U.; Sun, L.-B.; Balbuena, P. B.; Zhou, H.-C., *Chemical Communications* **2012,** *48* (80), 9995-9997.

52. Methane storage in advanced porous materials. Makal, T. A.; Li, J.-R.; Lu, W.; Zhou, H.-C., *Chemical Society Reviews* **2012,** *41* (23), 7761-7779.

53. Confinement of Metal–Organic Polyhedra in Silica Nanopores. Sun, L.-B.; Li, J.-R.; Lu, W.; Gu, Z.-Y.; Luo, Z.; Zhou, H.-C., *Journal Of The American Chemical Society* **2012,** *134* (38), 15923-15928.

54. Introduction of Functionalized Mesopores to Metal–Organic Frameworks via Metal–Ligand–Fragment Coassembly. Park, J.; Wang, Z. U.; Sun, L.-B.; Chen, Y.-P.; Zhou, H.-C., *Journal Of The American Chemical Society* **2012,** *134* (49), 20110-20116.

55. Highly porous metal-organic framework sustained with 12-connected nanoscopic octahedra. Lu, W.; Yuan, D.; Makal, T. A.; Wei, Z.; Li, J.-R.; Zhou, H.-C., *Dalton Transactions* **2013,** *42* (5), 1708-1714.

56. Linker extension through hard-soft selective metal coordination for the construction of a non-rigid metal-organic framework. Wei, Z.; Yuan, D.; Zhao, X.; Sun, D.; Zhou, H.-C., *Science China-Chemistry* **2013,** *56* (4), 418-422.

57. Generation and applications of structure envelopes for porous metal-organic frameworks. Yakovenko, A. A.; Reibenspies, J. H.; Bhuvanesh, N.; Zhou, H.-C., *Journal Of Applied Crystallography* **2013,** *46* (2), 346-353.

58. Interpenetration control in metal–organic frameworks for functional applications. Jiang, H.-L.; Makal, T. A.; Zhou, H.-C., *Coordination Chemistry Reviews* **2013,** *257* (15–16), 2232-2249.
59. Reversible Switching from Antiferro- to Ferromagnetic Behavior by Solvent-Mediated, Thermally-Induced Phase Transitions in a Trimorphic MOF-Based Magnetic Sponge System. Wriedt, M.; Yakovenko, A. A.; Halder, G. J.; Prosvirin, A. V.; Dunbar, K. R.; Zhou, H.-C., *Journal Of The American Chemical Society* **2013,** *135* (10), 4040-4050.
60. Structural design of porous coordination networks from tetrahedral building units. Zhang, M.; Chen, Y.-P.; Zhou, H.-C., *CrystEngComm* **2013**.
61. Selective gas adsorption and unique phase transition properties in a stable magnesium metal-organic framework constructed from infinite metal chains. Liu, Y.; Chen, Y.-P.; Liu, T.-F.; Yakovenko, A. A.; Raiff, A. M.; Zhou, H., *CrystEngComm* **2013**.
62. Building multiple adsorption sites in porous polymer networks for carbon capture applications. Lu, W.; Verdegaal, W. M.; Yu, J.; Balbuena, P. B.; Jeong, H.-K.; Zhou, H., *Energy & Environmental Science* **2013**.

Acronyms

MOF metal-organic framework
SBU secondary building unit
PCN porous coordination network
PPN porous polymer network
UMC unsaturated metal center
INS inelastic neutron scattering
NPD neutron powder diffraction
BET Brunauer-Emmett-Teller
PPN porous polymer frameworks
PXRD powder X-ray diffraction